

International Journal of Modern Physics A  
 © World Scientific Publishing Company

## PROBING THE PHASES OF QCD IN ULTRA-RELATIVISTIC NUCLEAR COLLISIONS

IVAN VITEV

*Los Alamos National Laboratory, Theory Division and Physics Division  
 Mail Stop H846, Los Alamos, NM 87545, USA*

Received 25 November 2004

The status of RHIC theory and phenomenology is reviewed with an emphasis on the indications for the creation of a new deconfined state of matter. The critical role of high energy nuclear physics in the development of theoretical tools that address various aspects of the QCD many body dynamics is highlighted. The perspectives for studying nuclear matter under even more extreme conditions at the LHC and the overlap with high energy physics is discussed.

*Keywords:* relativistic heavy ions, soft hadrons and thermalization, perturbative QCD, coherent power corrections, non-Abelian energy loss

### 1. Introduction

Quantum Chromodynamics and asymptotic freedom<sup>1</sup> predict the existence of a new state of matter<sup>2</sup>, the quark-gluon plasma (QGP), at exceedingly high temperatures and energy densities similar to the ones that characterized the first few microseconds after the Big Bang. The quest for such a deconfined state of QCD has led to the highly successful program at the Relativistic Heavy Ion Collider (RHIC) and will be an integral part of the program at the Large Hadron Collider (LHC). Recent theoretical developments have improved our understanding of the complex many-body dynamics in high energy nuclear collisions. Comparison between data and theory is suggestive of the creation of a deconfined state of QCD with energy density on the order of 100 times normal nuclear matter density. For a review of the RHIC experimental results see<sup>3</sup>.

### 2. Soft and Intermediate $p_T$ Hadrons

An economical description of the bulk particle production in  $A + A$  reactions can be achieved in the framework of the thermal model. All measured particle ratios at midrapidity from the  $\sqrt{s_{NN}} = 130, 200$  GeV  $Au + Au$  runs at RHIC are well reproduced with  $T_f \approx T_c \simeq 175$  MeV and  $\mu_B = 40, 30$  MeV, respectively<sup>4</sup>. Such approach, while instructive, does not carry information about the dynamical evolution prior to freeze-out. Constraining the initial conditions, relevant at the early

2 *Ivan Vitev*

stages of relativistic heavy ion collisions, requires the development and application of microscopic models.

*Relativistic hydrodynamics.* Differential particle distributions at low  $p_T$  can be calculated in the framework of relativistic hydrodynamics<sup>5</sup>, which assumes local thermal equilibrium and solves the energy-momentum and current conservation

$$\partial_\mu T^{\mu\nu}(x) = 0, \quad \partial_\mu j_i^\mu(x) = 0. \quad (1)$$

Additional constraints, necessary to determine the system Eq. (1), include, for example, ideal hydrodynamics and equation of state  $p = p(\epsilon)$  or a boost invariant Bjorken model. Good description of the  $p_T \leq 2 - 3$  GeV hadron spectra for  $\pi^\pm$ ,  $K^\pm$ ,  $p(\bar{p})$ ,  $\Lambda(\bar{\Lambda})$ ,  $\Omega, \dots$  can be obtained. However, the elliptic flow  $v_2$  of massive hadrons was shown to be much more sensitive to the choice of equation of state (EOS) with first order phase transition (preferred) versus hadronic EOS<sup>6</sup>. Traces of early partonic thermalization, as suggested by hydrodynamics, can also be found in the in the mean  $p_T$  fluctuations versus centrality<sup>7</sup>.

Recent hydrodynamic simulations have employed initial conditions motivated by gluon saturation phenomenology<sup>8</sup>. In  $A + A$  reaction this approach alleviates the problem with the transverse energy and the parton number in such models. However, it leaves an open question for  $p + A$  reactions where the hydrodynamic description is not applicable.

*Parton Coalescence.* Another microscopic approach to low and moderate  $p_T$  hadroproduction is the covariant Boltzmann transport<sup>9</sup>. The theory was shown to be applicable not only in  $A + A$  but also in  $p + A$  reactions<sup>10</sup> and has provided a good description of the rapidity density of hadrons  $dN^{ch}/dy$  and their transverse momentum distributions. The output of a partonic transport can be incorporated in the coalescence/recombination models that convolute the quark Wigner functions with the meson and baryon wavefunctions<sup>11</sup>. These predict scaling properties of the elliptic flow  $v_2$ <sup>12</sup>

$$v_2^M(p_T) = 2v_2^p(p_T/2), \quad v_2^B(p_T) = 3v_2^p(p_T/3) \quad (2)$$

at intermediate transverse momenta and enhanced baryon to meson ratios such as  $p(\bar{p})/\pi^\pm$  and  $\Lambda(\bar{\Lambda})/K^\mp$ . The energy loss of quarks and gluons plays an important role in the generation of the elliptic flow at the partonic level<sup>13</sup>. It also suppresses the perturbative high  $p_T$  hadron production and thus extends the region of possible non-perturbative contribution for baryons<sup>14</sup>. Coalescence models have been used to calculate the expected charm meson transverse momentum distributions and the charm meson and baryon elliptic flow<sup>15</sup>.

### 3. The Perturbative QCD Factorization Approach

In the nuclear environment, modifications to the QCD factorization approach<sup>16</sup> arise from the elastic, inelastic and coherent multiple scattering. These can be systematically incorporated in to the perturbative formalism<sup>17</sup>. For  $\ell + A$ ,  $p + A$

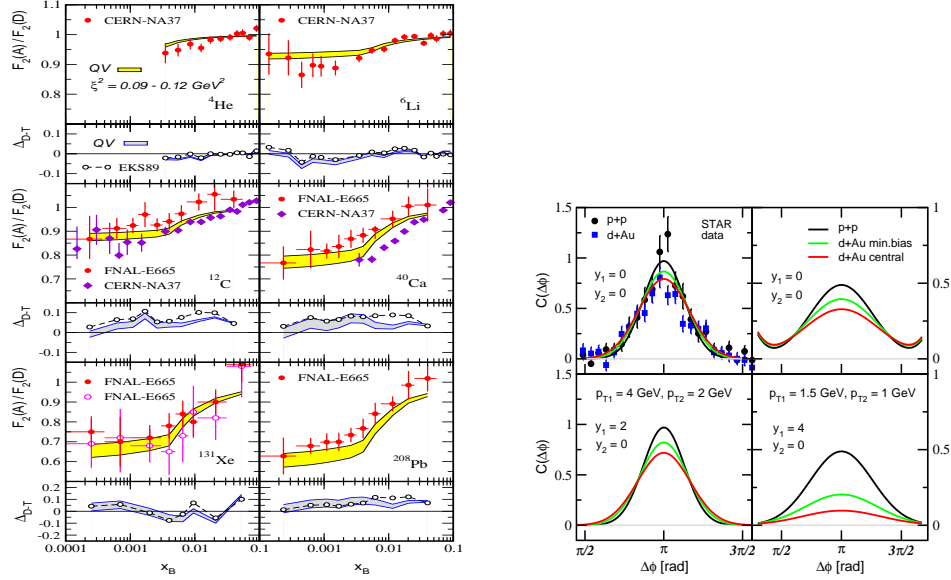


Fig. 1. Left panel from<sup>19</sup>: resummed QCD power corrections to nuclear shadowing in  $\ell + A$ , manifest in  $F_2(A)/F_2(D)$ . Right panel from<sup>21</sup>: modification of the away side correlation function  $C(\Delta\phi)$  versus rapidity, centrality and  $p_T$  from higher twist.

and  $A + A$  reactions their effect on experimental observables is summarized in Table 1. The relative importance of these distinct contributions in the different kinematic and density regimes is yet to be determined. Elastic scattering leads to a Cronin enhancement and a small broadening of the away side correlation function  $C(\Delta\phi) = (1/N_{trig})dN^{h_1h_2}/d\Delta\phi$ . These have been discussed in<sup>18</sup>.

*Coherent power corrections.* A class of corrections that can be naturally incorporated in the perturbative QCD factorization approach is associated with the power suppressed  $\sim 1/Q^n$ ,  $n \geq 1$  contributions. The higher twist terms are typically neglected in reactions with “elementary” nucleons for  $Q^2 \geq 1 \text{ GeV}^2$ . However, in the presence of nuclear matter such corrections can be enhanced by the large nuclear size  $\sim A^{1/3}$ .

The effective longitudinal interaction length probed by the virtual meson of

Table 1. Effect of elastic, inelastic and coherent multiple scattering on the transverse momentum distribution of hadrons in the perturbative regime.

Type of scattering	Transverse momentum dependence of the nuclear effect
<i>Elastic</i>	Suppression at low $p_T$ , enhancement at moderate $p_T$ , disappears at high $p_T$
<i>Inelastic</i>	Suppression at all $p_T$ , weak $p_T$ dependence, persists at high $p_T$
<i>Coherent</i>	Suppression at low $p_T$ , disappears at high $p_T$

4 Ivan Vitev

momentum  $q^\mu$  is characterized by  $1/xP$ . If the momentum fraction of an active initial-state parton  $x \ll x_c = 1/2m_N r_0 \sim 0.1$  with nucleon mass  $m_N$  and radius  $r_0$ , it could cover several Lorentz contracted nucleons of longitudinal size  $\sim 2r_0(m_N/P)$  in a large nucleus. Each of the soft interactions is characterized by a scale of power correction per nucleon  $\xi^2 \approx \frac{3\pi\alpha_s(Q)}{8r_0^2} \langle p|\hat{F}^2|p \rangle$  with the matrix element  $\langle p|\hat{F}^2|p \rangle = \frac{1}{2} \lim_{x \rightarrow 0} xG(x, Q^2)$ <sup>19</sup>. The multiple final state scattering of the struck quark generates a dynamical parton mass  $m_{\text{dyn}}^2 = \xi^2(A^{1/3} - 1)$  and a consequent rescaling in the value of Bjorken- $x$ <sup>19</sup>:

$$x_B \rightarrow x_B + x_B \frac{M_q^2}{Q^2} + x_B \frac{\xi^2(A^{1/3} - 1)}{Q^2} = x_B \left( 1 + \frac{M_q^2 + m_{\text{dyn}}^2}{Q^2} \right). \quad (3)$$

In Eq. (3)  $M_q$  is the physical mass of the quark in the final state.

In Ref. <sup>20</sup> next-to-leading order global analysis of the nuclear parton distributions (nPDFs) was shown to strongly disfavor more than 5% gluon shadowing. This result also suggests that the observed attenuation in the structure functions is a result of multiple final state scattering since any dynamical mechanism will predict an effect twice as large for gluons when compared to quarks,  $\xi^2 \rightarrow C_A/C_F \xi^2$ .

Application to nuclear shadowing in the DIS structure function  $F_2(A)$  is shown in the left panel of Fig. 1. The coherent nuclear enhanced power corrections in single and double inclusive hadron production in  $p + A$  reactions have been evaluated in<sup>21</sup>. The apparent suppression of the away side correlation function  $C(\Delta\phi) = (1/N_{\text{trig}})dN^{h_1 h_2}/d\Delta\phi$  is shown in the right hand side of Figure 1. As seen from Eq. (3), these modifications disappear at high  $p_T$ . It will be instructive to investigate the open charm production<sup>22</sup> including resummed power corrections. Additional discussion of nuclear shadowing and antishadowing in the light front approach can be found in<sup>23</sup>.

*Non-Abelian energy loss.* The most efficient mechanism that modifies the large transverse momentum hadroproduction in the presence of a hot and dense quark-gluon plasma is the medium induced gluon bremsstrahlung<sup>24</sup>. It leads to strong suppression of high- $p_T$  particles, known as jet quenching. Non-Abelian energy loss was also shown to be an effective attenuation mechanism in cold nuclear matter<sup>25</sup>.

The qualitative behavior of the energy loss as a function of the density and the size of the system can be calculated using the GLV approach<sup>27</sup>. To first order in opacity for static and 1+1D Bjorken expanding plasmas

$$\langle \Delta E \rangle \approx \begin{cases} \frac{9C_R\pi\alpha_s^3}{8} \rho^g \langle L \rangle^2 \ln \frac{2E}{\mu^2 \langle L \rangle}, & \text{static} \\ \frac{9C_R\pi\alpha_s^3}{4} \frac{1}{A_\perp} \frac{dN^g}{dy} \langle L \rangle \ln \frac{2E}{\mu^2 \langle L \rangle}, & 1+1D \end{cases}. \quad (4)$$

Application<sup>26</sup> of the QCD theory of energy loss to the single inclusive pion suppression and the attenuation of the away side dijet correlations is shown in Fig. 2. These persist, as shown by the calculation, to high  $p_T$ . For similar results see<sup>28</sup>.

Better experimental techniques may reveal the redistribution of the lost jet energy<sup>29</sup> in low frequency modes  $\geq \omega_{pl}$ . The quenching of charm and beauty

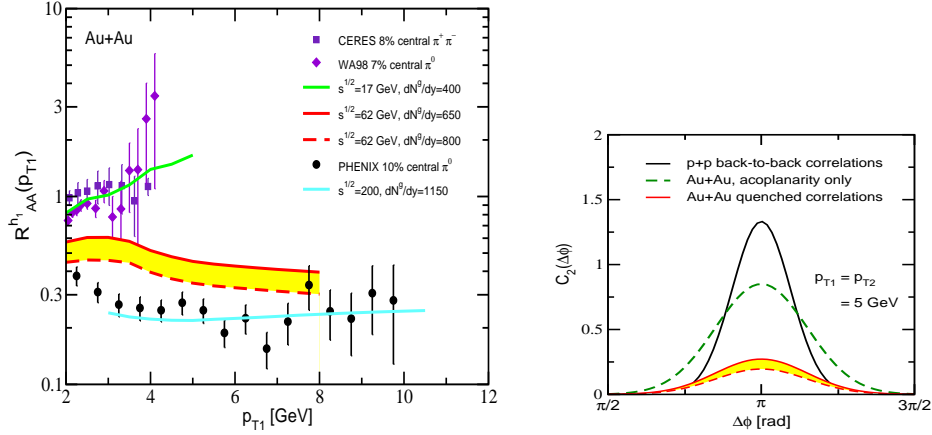


Fig. 2. Left panel from<sup>26</sup>: nuclear modification factor  $R_{AA}(p_T)$  at  $\sqrt{s_{NN}} = 17, 62$  and 200 GeV. Right panel from<sup>26</sup>: modification of the away side correlation function  $C(\Delta\phi)$  from energy loss at high  $p_T$ .

mesons<sup>30</sup> will provide a physical scale,  $m_c$  and  $m_b$ , relative to which the parameters of the medium can be reliably extracted.

#### 4. Conclusions

The complex dynamics of ultrarelativistic heavy ion reactions invites a variety of theoretical approaches, applicable in the different kinematic and density regimes, in the description of experimental observables. Consistent application of the models is required to better understand their strengths and limitation and to disentangle the distinct nuclear effects. At present, combined results from relativistic hydrodynamics and jet tomography suggest the creation of QGP at RHIC with initial energy density  $\epsilon \simeq 15 - 20$  GeV/fm<sup>3</sup>. The interactions in the plasma, however, remain strong and are consistent with the lattice expectation of  $\alpha_s \simeq 0.5$ <sup>31</sup>.

The upcoming RHIC runs and the LHC program will ensure the dominance of high  $p_T$  and jet physics<sup>32</sup> and will provide precision  $A + A$  data at  $\sqrt{s_{NN}} = 200 - 5500$  GeV<sup>33</sup>. This opens new possibilities for studying photon and dilepton tagged jets, heavy flavor and multiparticle correlations. For cold nuclear matter, a low energy  $p(d) + A$  run at RHIC will be a critical step in clarifying the relative importance of the nuclear effects summarized in Table 1.

*Acknowledgments.* I thank the organizers for the invitation to give this talk. This work is supported by the J.R. Oppenheimer Fellowship of the Los Alamos National Laboratory and by the US Department of Energy.

6 *Ivan Vitev***References**

1. D. J. Gross and F. Wilczek, Phys. Rev. D **9**, 980 (1974); H. D. Politzer, Phys. Rev. Lett. **30** (1973) 1346.
2. J. C. Collins and M. J. Perry, Phys. Rev. Lett. **34**, 1353 (1975).
3. J. L. Nagle, nucl-ex/0411027, these proceedings.
4. P. Braun-Munzinger *et al.*, Phys. Lett. B **518**, 41 (2001); D. Magestro,  $\sqrt{s_{NN}} = 200$  GeV update thereafter.
5. P. F. Kolb and U. Heinz, nucl-th/0305084; P. Huovinen, nucl-th/0305064; references therein.
6. P. Huovinen, P. F. Kolb and U. W. Heinz, Nucl. Phys. A **698**, 475 (2002).
7. S. Gavin, Phys. Rev. Lett. **92**, 162301 (2004); M. A. Aziz and S. Gavin, Phys. Rev. C **70**, 034905 (2004).
8. T. Hirano and Y. Nara, Nucl. Phys. A **743**, 305 (2004).
9. D. Molnar and M. Gyulassy, Phys. Rev. C **62**, 054907 (2000); B. Zhang, Comput. Phys. Commun. **109**, 193 (1998).
10. Z. W. Lin and C. M. Ko, Phys. Rev. C **68**, 054904 (2003).
11. R. J. Fries, J. Phys. G **30**, S853 (2004), references therein;
12. D. Molnar and S. A. Voloshin, Phys. Rev. Lett. **91**, 092301 (2003).
13. M. Gyulassy, I. Vitev and X. N. Wang, Phys. Rev. Lett. **86**, 2537 (2001); M. Gyulassy *et al.*, Phys. Lett. B **526**, 301 (2002).
14. I. Vitev and M. Gyulassy, Phys. Rev. C **65**, 041902 (2002).
15. V. Greco, C. M. Ko and R. Rapp, Phys. Lett. B **595**, 202 (2004); Z. W. Lin and D. Molnar, Phys. Rev. C **68**, 044901 (2003).
16. J. C. Collins, D. E. Soper and G. Sterman, Adv. Ser. Direct. High Energy Phys. **5** (1988) 1;
17. I. Vitev, to appear in J. Phys. G, hep-ph/0409297; hep-ph/0410045; J. W. Qiu and I. Vitev, hep-ph/0410218.
18. I. Vitev, Phys. Lett. B **562**, 36 (2003); J. W. Qiu and I. Vitev, Phys. Lett. B **570**, 161 (2003); M. Gyulassy, P. Levai and I. Vitev, Phys. Rev. D **66**, 014005 (2002).
19. J. W. Qiu and I. Vitev, Phys. Rev. Lett. in press, hep-ph/0309094; Phys. Lett. B **587**, 52 (2004).
20. D. de Florian and R. Sassot, Phys. Rev. D **69**, 074028 (2004).
21. J. W. Qiu and I. Vitev, hep-ph/0405068.
22. M. X. Liu, nucl-ex/0405034; these proceedings.
23. S. J. Brodsky, hep-ph/0411056; S. J. Brodsky and H. J. Lu, Phys. Rev. Lett. **64**, 1342 (1990).
24. M. Gyulassy *et al.*, nucl-th/0302077; R. Baier, D. Schiff and B. G. Zakharov, Ann. Rev. Nucl. Part. Sci. **50**, 37 (2000).
25. E. Wang and X. N. Wang, Phys. Rev. Lett. **89**, 162301 (2002).
26. I. Vitev, nucl-th/0404052; I. Vitev and M. Gyulassy, Phys. Rev. Lett. **89**, 252301 (2002);
27. M. Gyulassy, P. Levai and I. Vitev, Nucl. Phys. B **594**, 371 (2001); Phys. Rev. Lett. **85**, 5535 (2000); Nucl. Phys. B **571**, 197 (2000).
28. Q. Wang and X. N. Wang, nucl-th/0410049; A. Adil and M. Gyulassy, Phys. Lett. B **602**, 52 (2004).
29. S. Pal and S. Pratt, Phys. Lett. B **574**, 21 (2003).
30. M. Djordjevic and M. Gyulassy, Nucl. Phys. A **733**, 265 (2004).
31. O. Kaczmarek *et al.*, hep-lat/0406036; F. Znatow, these proceedings.
32. J. C. Collins and D. E. Soper, Nucl. Phys. B **193**, 381 (1981) [Erratum-ibid. B **213**, 545 (1983)].

33. H. Takai, J. Phys. G **30**, S1105 (2004); these proceedings; J. Liu, these proceedings.